Transition Metal Polyhydride Complexes. 10. Intramolecular Hydrogen Exchange in the Octahedral Iridium(III) Dihydrogen Dihydride Complexes $IrXH_2(\eta^2\text{-}H_2)(PR_3)_2$ (X = Cl, Br, I)

Shuhua Li,[†] Michael B. Hall,*[,†] Juergen Eckert,*[,‡] Craig M. Jensen,[§] and Alberto Albinati[⊥]

Contribution from the Department of Chemistry, Texas A&M University, College Station, Texas 77843, Los Alamos National Laboratory, Los Alamos, New Mexico 87545, Department of Chemistry, University of Hawaii, Honolulu, Hawaii 9682, and Dipartimento di Chimica Farmaceutica, Universita di Milano, Viale Abruzzi 42, I-20131, Milano, Italy

Received November 1, 1999. Revised Manuscript Received January 18, 2000

Abstract: Density functional calculations (B3LYP) on $IrXH_2(\eta^2\text{-}H_2)(PR_3)_2$ for X = Cl, Br, I and R = H, Me and inelastic neutron scattering studies for X = Cl, Br, I and R = Pr^i are used to elucidate the mechanisms for the intramolecular dihydrogen/hydride exchange. The two lowest energy processes are rotation of the dihydrogen ligand and oxidative addition of the dihydrogen to form an intermediate Ir(V) tetrahydride, which undergoes rapid reductive elimination to interchange the dihydrides and the dihydrogen. The use of PMe_3 as a model phosphine is essential to bring the calculated barriers for the dihydrogen/hydride interchange into agreement with the experimental observations. The activation energy for site exchange (1.9 kcal/mol) is found to be in excellent agreement with the experimental result obtained for X = Cl (1.5(2) kcal/mol), and the calculations show a slight decrease in this value from X = Cl to I. Comparison between calculated rotational barriers (0.4 to 0.7 kcal/mol) and experimental values obtained for $IrXH_2(\eta^2\text{-}H_2)(PR_3)_2$ (X = Cl, Br, I; R = Pr^i) (0.5 to 1.0 kcal/mol) also demonstrates that the quantitative estimate of the barrier to rotation requires PMe_3 as the minimal model ligand.

Introduction

The synthesis, characterization, structure, and reactivity of molecular hydrogen complexes[1−3] have been active areas since Kubas et al. discovered the first nonclassical dihydrogen complex.[1] Most η^2-H_2 complexes[1,4−9] have been characterized by combinations of several experimental methods such as IR and NMR spectroscopy and X-ray and neutron diffraction. Theoretical calculations[7d,e,10−14] have also been carried out to substantiate the presence or absence of nonclassical H_2 ligands for many transition metal polyhydride complexes. Increasingly, one finds both experimental and theoretical studies on the

[†]Texas A&M University.
[‡]Los Alamos National Laboratory.
[§] University of Hawaii.
[⊥] Universita di Milano.

(1) Kubas, G. J.; Ryan, R. R.; Swanson, B. I.; Vergamini, P. J.; Wasserman, H. *J. Am. Chem. Soc.* **1984**, *106*, 451.
(2) (a) Kubas, G. J. *Acc. Chem. Res.* **1988**, *21*, 129. (b) Crabtree, R. H. *Acc. Chem. Res.* **1990**, 23, 95.
(3) (a) Esteruelas, M. A.; Oro, L. A. *Chem. Rev.* **1998**, *98*, 577. (b) Heinekey, D. M.; Oldham, W. J., Jr. *Chem. Rev.* **1993**, *93*, 913. (c) Jessop, P. G.; Morris, R. H. *Coord. Chem. Rev.* **1992**, *121*, 155. (d) Maseras, F.; Lledós, A.; Clot, E.; Eisenstein, O. *Chem. Rev.* **2000**, *100*, 601.
(4) (a) Kubas, G. J.; Ryan, R. R.; Wroblewski, D. *J. Am. Chem. Soc.* **1986**, *108*, 1339. (b) Kubas, G. J.; Unkefer, C. J.; Swanson, B. J.; Fukushima, E. *J. Am. Chem. Soc.* **1986**, *108*, 7000. (c) Khalsa, G. R. K.; Kubas, G. J.; Unkefer, C. J.; Van der Sluys, L. S.; Kubat-Martin, K. A. *J. Am. Chem. Soc.* **1990**, *112*, 3855.
(5) (a) Morris, R. H.; Sawyer, J. F.; Shiralian, M.; Zubkowski, J. D. *J. Am. Chem. Soc.* **1985**, *107*, 5581. (b) Ricci, J. S.; Koetzle, T. F.; Bautista, M. T.; Hofstede, T. M.; Morris, R. H.; Sawyer, J. F. *J. Am. Chem. Soc.* **1989**, *111*, 8823. (c) Earl, K. A.; Jia, G.; Maltby, P. A.; Morris, R. H. *J. Am. Chem. Soc.* **1991**, *113*, 3027. (d) Bautista, M. T.; Cappellani, E. P.; Drouin, S. D.; Morris, R. H.; Schweitzer, C. T.; Sella, A.; Zubkowski, J. D. *J. Am. Chem. Soc.* **1991**, *113*, 4876. (e) Bautista, M. T.; Earl, K. A.; Morris, R. H.; Sella, A. *J. Am. Chem. Soc.* **1987**, *109*, 3780. (f) Van Der Sluys, L. S.; Eckert, J.; Eisenstein, O.; Hall, J. H.; Huffman, J. C.; Jackson, S. A.; Koetzle, T. F.; Kubas, G. J.; Vergamini, P. J.; Caulton, K. G. *J. Am. Chem. Soc.* **1990**, *112*, 4831. (g) Eckert, J.; Blank, H.; Bautista, M. T.; Morris, R. H. *Inorg. Chem.* **1990**, *29*, 747. (h) Sweany, R. L. *J. Am. Chem. Soc.* **1985**, *107*, 2374. (i) Upmacis, R. K.; Poliakoff, M.; Turner, J. *J. Am. Chem. Soc.* **1986**, *108*, 3645.
(6) (a) Guari, Y.; Sabo-Etienne, S.; Chaudret, B. *J. Am. Chem. Soc.* **1998**, *120*, 4228. (b) Oldham, W. J., Jr.; Hinkle, A. S.; Heinekey, D. M. *J. Am. Chem. Soc.* **1997**, *119*, 11028.
(7) (a) Luther, T. A.; Heinekey, D. M. *Inorg. Chem.* **1998**, *37*, 127. (b) Heinekey, D. M.; Radzewich, C. E.; Voges, M. H.; Schomber, B. M. *J. Am. Chem. Soc.* **1997**, *119*, 4172. (c) Bianchini, C.; Moneti, S.; Peruzzini, M.; Vizza, F. *Inorg. Chem.* **1997**, *36*, 5818. (d) Bianchini, C.; Masi, D.; Peruzzini, M.; Casarin, M.; Maccato, C.; Rizzi, G. A. *Inorg. Chem.* **1997**, *36*, 1061. (e) Barea, G.; Esteruelas, M. A.; Lledós, A.; López, A. M.; Tolosa, J. I. *Inorg. Chem.* **1998**, *37*, 5033.
(8) (a) Crabtree, R. H.; Lavin, M. *J. Chem. Soc., Chem. Commun.* **1985**, *794*, 1661. (b) Crabtree, R. H.; Lavin, M.; Bonneviot, L. *J. Am. Chem. Soc.* **1986**, *108*, 4032. (c) Luo, X. L.; Crabtree, R. H. *J. Am. Chem. Soc.* **1990**, *112*, 6912.
(9) (a) Mediati, M.; Tachibana, G. N.; Jensen, C. M. *Inorg. Chem.* **1990**, *29*, 3. (b) Mediati, M.; Tachibana, G. N.; Jensen, C. M. *Inorg. Chem.* **1992**, *31*, 1827. (c) Eckert, J.; Jensen, C. M.; Koetzle, T. F.; Husebo, T. L.; Nicol, J.; Wu, P. *J. Am. Chem. Soc.* **1995**, *117*, 7271.
(10) Maseras, F.; Duran, M.; Lledós, A.; Bertran, J. *J. Am. Chem. Soc.* **1992**, *114*, 2922.
(11) (a) Lin, Z.; Hall, M. B. *J. Am. Chem. Soc.* **1992**, *114*, 2928. (b) Lin, Z.; Hall, M. B. *J. Am. Chem. Soc.* **1992**, *114*, 6102. (c) Lin, Z.; Hall, M. B. *Coord. Chem. Rev.* **1994**, *135/136*, 845. (d) Lin, Z.; Hall, M. B. *J. Am. Chem. Soc.* **1994**, *116*, 4446. (e) Bayse, C. A.; Hall, M. B.; Pleune, B.; Poli, R. *Organometallics* **1998**, *17*, 4309. (f) Bayse, C. A.; Couty, M.; Hall, M. B. *J. Am. Chem. Soc.* **1996**, *118*, 8916.
(12) Burdett, J. K.; Pourian, M. R. *Organometallics* **1987**, *6*, 1684.
(13) (a) Eckert, J.; Kubas, G. J.; Hall, J. H.; Hay, P. J.; Boyle, C. M. *J. Am. Chem. Soc.* **1990**, *112*, 2324. (b) Rodriguez, V.; Sabo-Etienne, S.; Chaudret, B.; Thoburn, J.; Ulrich, S.; Limbach, H.; Eckert, J.; Barthelat, J.; Hussein, K.; Marsden, C. J. *Inorg. Chem.* **1998**, *37*, 3475.
(14) Riehl, J. F.; Pelissier, M.; Eisenstein, O. *Inorg. Chem.* **1992**, *31*, 3344.

10.1021/ja993877a CCC: $19.00
Published on Web 03/10/2000

Scheme 1

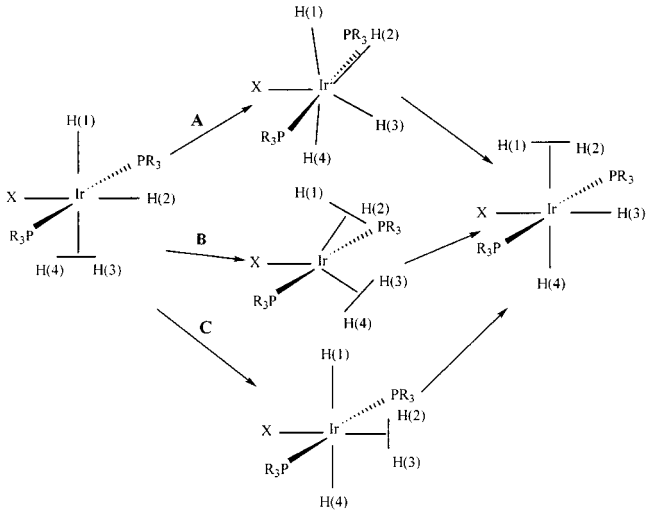

reactivity of polyhydride complexes, especially intramolecular site exchange between molecular hydrogen and hydride ligands in complexes where both ligands coexist.[6,10,11,15,16] This intramolecular process has been observed experimentally for systems such as *cis*-$[Fe(PR_3)_4H(\eta^2\text{-}H_2)]^+$,[5b] $Cr(CO)_4(\eta^2\text{-}H_2)_2$,[5i] $RuH(H_2)(Ph\text{-}py)(PPr^i_3)_2$,[6a] $[TpM(PR_3)(H_2)H]^+$ (M = Ir, Rh),[6b] $[Ir(bq)(PCy_3)_2H(\eta^2\text{-}H_2)]^+$,[8b] $[ReH_4(CO)(PMe_2Ph)_3]^+$,[8c] and $[Cp^*MoH_4(\eta^2\text{-}H_2)(PMe_3)]^+$.[11e] With respect to the site exchange mechanism, ab initio calculations[10,11d−f] have shown the possibilities of a variety of rearrangement mechanisms. For example, a reductive-elimination/oxidative-addition (REOA) pathway through a bis(dihydrogen) intermediate was proposed for the $[ReH_4(CO)(PMe_2Ph)_3]^+$ complex,[11d] but for the *cis*-$[Fe(PR_3)_4H(\eta^2\text{-}H_2)]^+$ and $[Cp^*MoH_4(\eta^2\text{-}H_2)(PMe_3)]^+$ complexes, the preferred reaction pathway is to go through a "trihydrogen anion" transition state.[10,11e]

The rapid exchange between the dihydrogen and hydride ligands in the complexes $IrXH_2(\eta^2\text{-}H_2)(PPr^i_3)_2$ (X = Cl, Br, I) was observed by solution NMR spectroscopy.[9] A subsequent solid-state ^1H NMR study[15] revealed that this exchange persists down to the lowest temperature reached in the experiment (77 K) and that its barrier in the complex $IrClH_2(\eta^2\text{-}H_2)(PPr^i_3)_2$ is "substantially under 3 kcal/mol". It was also determined in this study that the metal-bound hydrogens remain as distinct pairs which do not cross the Cl−Ir−P plane. This observation immediately excluded the direct proton-transfer approach (pathway C in Scheme 1) as a possible mechanism. However, this result failed to distinguish between the two possible mechanisms denoted as pathways A and B in Scheme 1. Pathway A is the oxidative-addition/reductive-elimination (OARE) process, in which the hydrogen molecule oxidatively adds to the metal, leading to a tetrahydride intermediate, and then two hydride ligands reductively eliminate to regenerate the molecular hydrogen ligand. Pathway B involves a bis(dihydrogen) intermediate, which is obviously a REOA process.

In addition to the dihydrogen−hydride exchange observed by NMR, rotational barriers of 0.5 and 1.0 kcal/mol have been previously derived[17] from observations of rotational transitions of the dihydrogen ligand by inelastic neutron scattering (INS) for X = Cl[18] and I,[9c] respectively. Coupling between dihydrogen rotation and hydrogen−hydride exchange may also play a role in the experimental observations[9c,18] because the energies involved for the two processes apparently are relatively close in magnitude. INS is extremely sensitive to the height of the rotational barrier because the rotational tunnel splitting of the ground state has an exponential dependence of the barrier height.[17] The theoretical calculation of rotational barriers is a sensitive test to the accuracy of the calculated metal−H_2 interaction because describing the weak metal−H_2 interaction in transition metal complexes is difficult for available theoretical methods.[5f,13]

This paper presents a combination of theoretical and experimental studies on hydrogen exchange in closely related complexes. We report calculations by density functional theory (DFT)[19] on the model systems $IrXH_2(\eta^2\text{-}H_2)(PR_3)_2$ (X = Cl, Br, I; R = H, Me) to determine the most favorable pathways and corresponding activation parameters for the dihydrogen/hydride exchange and the rotational barriers of the dihydrogen ligand. We also report new results of the barrier to rotation for the compound X = Br and R = Pr^i, and the first experimental observation by inelastic neutron scattering of quasielastic scattering attributable to the dihydrogen/hydride site exchange and its associated activation energy for the compound X = Cl and R = Pr^i. Comparisons are made between the calculated barriers and the new and previously reported experimental values.

Experimental and Computational Section

Inelastic neutron scattering data on $IrXH_2(\eta^2\text{-}H_2)(PPr^i_3)_2$ (X = Cl, Br, I) were collected on the cold neutron time-of-flight spectrometers IN5 at the Institute Laue-Langevin (Grenoble, France) and MIBEMOL at the Laboratoire Leon-Brillouin (Saclay, France) over the temperature range from 1.7 to 250 K. Approximately 1 g of each compound was sealed in quartz sample holders, with a geometry of an annular cylinder, under hydrogen atmosphere. Incident wavelengths between 2 and 4.5 Å were used to cover different frequency ranges. Data reduction and analyses were carried out using standard routines available at the ILL.

All the calculations on the model systems $IrXH_2(\eta^2\text{-}H_2)(PR_3)_2$ (X = Cl, Br, I; R = H, Me) have been performed with the Gaussian 94 package[20] by density functional theory (specifically B3LYP) and by the second-order Møller−Plesset (MP2) method[21] (X = I only). The exchange potential in B3LYP is the three-parameter hybrid functional of Becke[22] and the correlation potential is due to Lee, Yang, and Parr.[23] The Hay−Wadt relativistic effective core potentials (ECPs)[24] for iridium, phosphorus, and the halides (X = Cl, Br, I) were employed in all MP2 and DFT calculations. In the ECP for Ir, the 5s and 5p orbitals were treated explicitly along with the 5d, 6s, and 6p valence orbitals.

The basis set for P and the halides X (X = Cl, Br, I) was the standard

(15) Wisiniewski, L. L.; Mediati, M.; Jensen, C. M.; Zilm, K. W. *J. Am. Chem. Soc.* **1993**, *115*, 7533.

(16) Esterulas, M. A.; Herrero, J.; López, A. M.; Oro, L. A.; Schultz, M.; Werner, H. *Inorg. Chem.* **1992**, *31*, 4013.

(17) Eckert, J.; Kubas, G. J. *J. Phys. Chem.* **1993**, *97*, 2378.

(18) Eckert, J.; Jensen, C. M.; Jones, G.; Clot, E.; Eisenstein, O. *J. Am. Chem. Soc.* **1993**, *115*, 11056.

(19) Parr, R. G.; Yang, W. *Density-functional theory of atoms and molecules*; Oxford University Press: Oxford, 1989.

(20) Frisch, M. J.; Trucks, G. W.; Schlegel, H. B.; Gill, P. M. W.; Johnson, B. G.; Robb, M. A.; Cheeseman, J. R.; Keith, T.; Petersson, G. A.; Montgomery, J. A.; Raghavachari, K.; Al-Laham, M. A.; Zakrzewski, V. G.; Ortiz, J. V.; Foresman, J. B.; Peng, C. Y.; Ayala, P. Y.; Chen, W.; Wong, M. W.; Andres, J. L.; Replogle, E. S.; Gomperts, R.; Martin, R. L.; Fox, D. J.; Binkley, J. S.; Defrees, D. J.; Baker, J.; Stewart, J. P.; Head-Gordon, M.; Gonzalez, C.; Pople, J. A. *Gaussian 94*, Revision B.3; Gaussian Inc.: Pittsburgh, PA, 1994.

(21) (a) Møller, C.; Plesset, M. S. *Phys. Rev.* **1934**, 46, 618. (b) Hehre, W. J.; Radom, L.; Schleyer, P. v. R.; Pople, J. A. *Ab Initio Molecular Orbital Theory*; Wiley: New York, 1986.

(22) (a) Becke, A. D. *Phys. Rev.* **1988**, *A38*, 3098. (b) Becke, A. D. *J. Chem. Phys.* **1993**, *98*, 1372. (c) Becke, A. D. *J. Chem. Phys.* **1993**, *98*, 5648.

(23) Lee, C.; Yang, W.; Parr, R. G. *Phys. Rev.* **1988**, *B37*, 785.

(24) (a) Hay, P. J.; Wadt, W. R. *J. Chem. Phys.* **1985**, *82*, 299. (b) Wadt, W. R.; Hay, P. J. *J. Chem. Phys.* **1985**, *82*, 284.

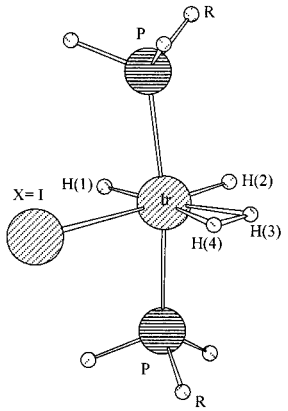

	R=H	R=Me	R=Pr^i
Ir-I	2.846	2.882	2.770(4)
Ir-P	2.319	2.353	2.336(4)[a]
Ir-H(1)	1.587	1.593	1.579(6)
Ir-H(2)	1.594	1.592	1.589(6)
Ir-H(3)	1.793	1.770	1.748(7)
Ir-H(4)	1.804	1.783	1.764(7)
H(3)-H(4)	0.847	0.862	0.856(9)

[a] Average of two values.

Figure 1. The B3LYP/BS4-optimized geometry for the molecular hydrogen complex $IrIH_2(\eta^2\text{-}H_2)(PR_3)_2$ (R = H, Me) and comparison with the neutron diffraction structure of $IrIH_2(\eta^2\text{-}H_2)(PPr^i_3)_2$.

Table 1. Selected B3LYP Optimized Geometrical Parameters of $IrIH_2(\eta^2\text{-}H_2)(PR_3)_2$ (R = H, Me) with Four Different Basis Sets and Comparison with a Related Neutron Diffraction Structure Obtained for $IrIH_2(\eta^2\text{-}H_2)(PR_3)_2$ (R = Pr^i)[a,b]

	R = H				R = Me		R = Pr^i
	BS1[c]	BS2	BS3	BS4	BS1[c]	BS4	exptl[d]
Ir−I	2.861	2.841	2.863	2.846	2.896	2.882	2.770(4)
Ir−P	2.320	2.318	2.321	2.319	2.360	2.353	2.336(4)
Ir−H(1)	1.573	1.585	1.574	1.587	1.578	1.593	1.579(6)
Ir−H(2)	1.591	1.593	1.588	1.594	1.586	1.592	1.589(6)
Ir−H(3)	1.855	1.807	1.834	1.793	1.822	1.770	1.748(7)
Ir−H(4)	1.863	1.818	1.844	1.804	1.838	1.783	1.764(7)
H(3)−H(4)	0.819	0.839	0.827	0.847	0.830	0.862	0.856(9)

[a] See Figure 1 for the numbering of atoms. [b] See the text for the definitions of four basis sets. [c] As discussed in ref 31. [d] Neutron diffraction structure for $IrIH_2(\eta^2\text{-}H_2)(PR_3)_2$ (R = Pr^i) from ref 9c.

LANL2DZ[25]/Gaussian 94 augmented by a polarization d function.[26] A STO-3G basis set[27] was used for those hydrogen atoms uncoordinated to the metal (i.e., in PH_3 and PMe_3) and the carbon atoms (in PMe_3). The basis sets for Ir and those metal-coordinated dihydrogen and hydrides deserve special attention because their selection has considerable influence on the calculated barriers of site exchange and rotation of the dihydrogen ligand. For Ir, it has been shown that a double-ζ basis set (341/541/21), where the two outermost 6p functions of the "standard" LANL2DZ (341/321/21) have been replaced by a (41) split of the optimized 6p function from Couty and Hall,[28] gives better descriptions for the bonding between Ir and its ligands. Similarly, we have examined two choices for the basis set of metal-coordinated hydrogens: 6-31G(p)[29] and 6-311G(p).[30] Thus, we have four different combinations for Ir and metal-bound hydrogen basis sets: BS1 (LANL2DZ, 6-31G(p)), BS2 (Modified LANL2DZ, 6-31G(p)), BS3 (LANL2DZ, 6-311G(p)), and BS4 (Modified LANL2DZ, 6-311G(p)). To determine the difference among these four basis sets, we have compared the B3LYP-optimized geometries of $IrIH_2(\eta^2\text{-}H_2)(PR_3)_2$ (R = H, Me) obtained with these basis sets to the related experimental parameters for $IrIH_2(\eta^2\text{-}H_2)(PR_3)_2$ (R = Pr^i). The results displayed in Figure 1 and listed in Table 1 clearly show that BS4 provides the best descriptions for the geometries of the model systems $IrIH_2(\eta^2\text{-}H_2)(PR_3)_2$ (R = H, Me) if the neutron diffraction structure of $IrIH_2(\eta^2\text{-}H_2)(PR_3)_2$ (R = Pr^i)[9c] is used to calibrate the calculated geometries. It is easy to see from Figure 1 that, with the exception of the Ir−I distance, the agreement between experimental geometrical parameters and calculated ones with BS4 is excellent, especially when PMe_3 is used as a model phosphine. There is a significant overall improvement for the geometries of $IrIH_2(\eta^2\text{-}H_2)(PR_3)_2$ (R = H, Me) when the basis sets for Ir and metal-bound hydrogens are changed from BS1 to BS4 (see Table 1). In $IrIH_2(\eta^2\text{-}H_2)(PMe_3)_2$ the H(3)−H(4) distance lengthens from 0.830 to 0.862 (vs 0.856(9) Å experimental) and even more dramatically the Ir−H(3) and Ir−H(4) bond lengths shorten from 1.822 and 1.838 to 1.770 and 1.783 Å, respectively, which are very close to the corresponding experimental values of 1.748(7) and 1.764(7) Å. In addition, a comparison between BS1 and BS2 listed in Table 1 for R = H reveals that the optimized 6p function alone significantly improves the Ir−H_2 bonding description. On the basis of these results, we again recommend the use of the modified LANL2DZ basis set by Couty and Hall[28] in studying transition metal complexes.

Previous studies[31] using BS1 resulted in a conclusion that the MP2 level of theory gives a little better description than B3LYP for the same molecular hydrogen complexes. However, this is not the case for the larger basis sets. In the MP2 optimizations for $IrIH_2(\eta^2\text{-}H_2)(PH_3)_2$, we found that the molecular hydrogen complex is no longer a minimum with the best basis set, BS4. This result reminds us that the MP2 method often overestimates the Ir−H_2 interaction[31] and favors the oxidative-addition product; accordingly, the corresponding tetrahydride complex was found as a local minimum by MP2/BS4. For this reason, only the B3LYP method is used in subsequent optimizations of the species involved in the dihydrogen/hydride exchange and rotation of the molecular hydrogen of $IrXH_2(\eta^2\text{-}H_2)(PR_3)_2$ (X = Cl, Br, I; R = H, Me). Likewise, the BS4 basis set is used for all geometry optimizations. We also present the relative energies of some species calculated with other electron correlation methods such as MP2, MP3,[21] MP4(SDQ),[21] CISD,[32] and CCSD[33] at the B3LYP/BS4 geometries and with another basis set (BS5), which is BS4 augmented with an f polarization function on Ir.[34]

The nature of the stationary points was checked by separate frequency calculations for all species with R = H. In other cases, only the updated Hessian matrix was used to characterize the stationary points.

Results and Discussion

This section begins by describing the optimized structures of $IrXH_2(\eta^2\text{-}H_2)(PR_3)_2$ (X = Cl, Br, I; R = H, Me). Next, the rotation of the dihydrogen ligand is described briefly, and finally, the dihydrogen/hydride exchange process is described in greater detail. Experimental and theoretical results are combined for clarity.

Structures of $IrXH_2(\eta^2\text{-}H_2)(PR_3)_2$ (X = Cl, Br, I; R = H, Me). As shown in the Experimental and Computational Section, B3LYP calculations with basis set BS4 are necessary for accurate results in these complexes. In Table 2 we tabulate the calculated (B3LYP/BS4) geometrical parameters of the molecular hydrogen complexes $IrXH_2(\eta^2\text{-}H_2)(PR_3)_2$ (X = Cl, Br, I; R = H, Me) (see Figure 1 for the numbering of atoms). Frequency calculations have verified that the corresponding molecular hydrogen compound is a local minimum for each halide with either PH_3 or PMe_3. Interestingly, although the distances involving dihydrogen and the hydrides are similar for the series Cl, Br, and I, one can clearly see that the bond distances Ir−H(3) and Ir−H(4) are slightly shortened and simultaneously the H(3)−H(4) bond is slightly lengthened along the series. This trend, which is seen for both PH_3 and PMe_3, is

(25) LANL2DZ: Dunning D95 basis sets on first row, Los Alamos ECP plus double-ζ basis sets on Na−Bi.
(26) Höllwarth, A.; Böhme, M.; Dapprich, S.; Ehlers, A. W.; Gobbi, A.; Jonas, V.; Köhler, K. F.; Stegmann, R.; Veldkamp, A.; Frenking, G. *Chem. Phys. Lett.* **1993**, *208*, 237.
(27) Hehre, W. J.; Stewart, R. F.; Pople, J. A. *J. Chem. Phys.* **1969**, *51*, 2657.
(28) Couty, M.; Hall, M. B. *J. Comput. Chem.* **1996**, *17*, 1359.
(29) Harihan, P. C.; Pople, J. A. *Theor. Chim. Acta* **1973**, *28*, 213.
(30) Krishnan, R.; Frisch, M. J.; Pople, J. A. *J. Chem. Phys.* **1980**, *72*, 4244.
(31) Clot, E.; Eisenstein, O. *J. Phys. Chem. A* **1998**, *102*, 3592.
(32) Pople, J. A.; Binkley, J. S.; Seeger, R. *Int. J. Quantum. Chem. Symp.* **1976**, *10*, 1.
(33) (a) Cizek, J. *Adv. Chem. Phys.* **1969**, *14*, 35. (b) Purvis, G. D.; Bartlett, R. J. *J. Chem. Phys.* **1982**, *76*, 1910.
(34) Ehlers, A. W.; Böhme, M.; Dapprich, S.; Gobbi, A.; Höllwarth, A.; Jonas, V.; Köhler, K. F.; Stegmann, R.; Veldkamp, A.; Frenking, G. *Chem. Phys. Lett.* **1993**, *208*, 111.

Table 2. Selected B3LYP/BS4-Optimized Geometrical Parameters of $IrXH_2(\eta^2\text{-}H_2)(PR_3)_2$ (X = Cl,Br, I; R = H, Me)[a]

	R = H			R = Me		
	X = Cl	X = Br	X = I	X = Cl	X = Br	X = I
Ir−X	2.524	2.676	2.846	2.561	2.712	2.882
Ir−P	2.316	2.317	2.319	2.349	2.351	2.353
Ir−H(1)	1.585	1.586	1.587	1.591	1.591	1.593
Ir−H(2)	1.593	1.593	1.594	1.592	1.591	1.592
Ir−H(3)	1.805	1.800	1.793	1.775	1.773	1.770
Ir−H(4)	1.820	1.813	1.804	1.795	1.790	1.783
H(3)−H(4)	0.836	0.841	0.847	0.853	0.857	0.862

[a] See Figure 1 for the numbering of atoms.

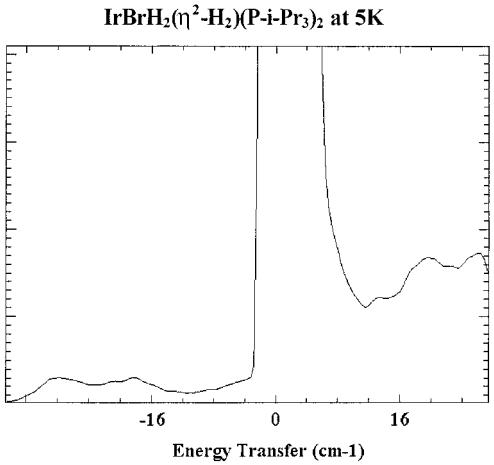

Figure 2. INS spectrum for $T = 5$ K of $IrBrH_2(\eta^2\text{-}H_2)(PPr^i_3)_2$ collected on IN5 at the ILL with an incident wavelength of 4 Å.

easily understandable because as the halide becomes less electronegative, the electron density on Ir increases, the back-donation into the H_2 σ^* orbital increases, the Ir−H_2 interaction strengthens, and the H−H bond lengthens. On the other hand, we note that for each halide the dihydrogen ligand is bonded to the metal more strongly with PMe_3 than with PH_3, and as shown in the Experimental and Computational Section, the former is a better choice for mimicking the experimental phosphine geometry.

Rotation of the Molecular Hydrogen. At very low temperatures the spectrum of the Cl and I analogues consists of rather broad rotational tunneling transitions at approximately ±20 and ±6 cm^{-1}, respectively, as previously reported.[9c,18] The spectrum of the Br complex, however, shows a pair of such transitions (Figure 2) at ±19 and ±29 cm^{-1}. The origin of this splitting is likely to be the result of the presence of two inequivalent molecules in the crystal, which may give rise to different barriers to rotation at each complex. This splitting could also arise from the presence of the two distinct isomers in the absence of the rapid interconversion at low temperatures. However, we consider the former explanation to be more likely, because a similar effect was in fact observed in $W(CO)_3(\eta^2\text{-}H_2)(PPr^i_3)_2$[35] and appears to be qualitatively in accord with disorder found in the phosphine ligands. With increasing temperature, however, the intensity of the peak at 29 cm^{-1} in the Br analogue shifts into the peak at 19 cm^{-1} and by about 40 K only the latter remains. We have, therefore, in the following discussion taken the transition at 19 cm^{-1} to be characteristic of dihydrogen in the Br complex.

A value of the barrier to rotation can be derived from the observation of rotational tunnel splitting of the librational ground state if one assumes that the reorientation of the dihydrogen ligand occurs in a plane perpendicular to the M−H_2 rotation axis with a double-minimum potential[35] and a knowledge of the rotational constant *B*, i.e., the H−H distance, from other experiments such as neutron diffraction or solid state NMR. We determine *B* with the aid of *d*(HH) from neutron diffraction results, namely 0.82 and 0.86 Å for the Br and I analogues, respectively.[9c,36] For the Cl complex *B* was taken to be a variable[18] and determined from the observed rotational transitions to be 0.78 Å. A more elaborate analysis[37] of the rotational barrier was recently carried out for the Cl analogue with the same result for *d*(HH). With these values and under the simple assumption of a 2-fold rotational barrier we find $V_2 = 0.51(3)$, 0.48(3), and 1.00(4) kcal/mol for the Cl, Br, and I complexes, respectively.

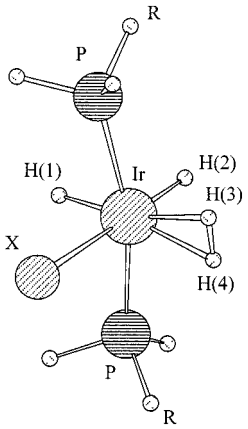

X=Cl	R=H	R=Me
Ir-X	2.520	2.558
Ir-P	2.317	2.349
Ir-H(1)	1.580	1.590
Ir-H(2)	1.592	1.591
Ir-H(3)	1.843	1.797
Ir-H(4)	1.843	1.797
H(3)-H(4)	0.817	0.842

Figure 3. The B3LYP/BS4-optimized geometry for the transition state of the rotation of the dihydrogen ligand in $IrXH_2(\eta^2\text{-}H_2)(PR_3)_2$ (X = Cl; R = H, Me).

Experimental measurements on the rotational barrier of the dihydrogen ligand in molecular hydrogen complexes provide a considerable amount of insight into the dihydrogen−metal interaction.[5f,g,9c,18] Comparison between measured and calculated rotational barriers of the dihydrogen ligand is expected to provide a sensitive test on the accuracy of the theoretical methods. In prior work, quantitative predictions of the rotational barriers have met with only fair success.[5f,13] For instance, with X = Cl and R = H the rotational barrier was calculated to be 2.2 kcal/mol at the MP2//RHF level,[18] a value significantly larger than the corresponding experimental value. However, our present calculations, vida infra, show that the rotational barriers for the experimental systems can be very well reproduced at the B3LYP/BS4 level when PMe_3 is used as the phosphine.

Figure 3 shows the B3LYP/BS4-optimized transition state geometry for the dihydrogen rotation in $IrClH_2(\eta^2\text{-}H_2)(PR_3)_2$ (R = H, Me). Selected geometrical parameters of the transition state for the whole halide series are displayed in Table 3. For each halide, the replacement of PH_3 by PMe_3 introduces a fairly large change in the geometry of the coordinated H_2 ligand. Since PMe_3 is a stronger electron donor than PH_3,[38] the metal with PMe_3 has more electrons available for π back-donation to the σ^* orbital of the molecular hydrogen, which strengthens the Ir−H_2 interaction. This ligand effect is reflected in the Ir−H(3) and Ir−H(4) bonds which are shorten by 0.04 Å and simultaneously in the H(3)−H(4) distance which is elongated by about 0.02 Å for each halide. In addition, one can see that for each halide the dihydrogen ligand is bonded to the metal more weakly

(35) Eckert, J. *Spectrochim. Acta A* **1992**, *48*, 363.

(36) Albinati, A.; Jensen, C. M.; Koetzle, T. F.; Klooster, W.; Mason, S. A.; Eckert, J. Manuscript in preparation, 1999.

(37)) Clot, E.; Eckert, J. *J. Am. Chem. Soc.* **1999**, *121*, 8855.

(38) (a) Song, J.; Hall, M. B.*J. Am. Chem. Soc.* **1993**, *115*, 327. (b) Jacobsen, H.; Berke, H. *Chem. Eur. J.* **1997**, *3*, 881.

Table 3. Selected B3LYP/BS4 Optimized Geometrical Parameters for the Rotational Transition States of the Dihydrogen Ligand in $IrXH_2(\eta^2\text{-}H_2)(PR_3)_2$ (X = Cl, Br, I; R = H, Me)[a]

	R = H			R = Me		
	X = Cl	X = Br	X = I	X = Cl	X = Br	X = I
Ir−X	2.520	2.671	2.843	2.558	2.712	2.882
Ir−P	2.317	2.318	2.320	2.349	2.352	2.354
Ir−H(1)	1.580	1.580	1.582	1.590	1.590	1.591
Ir−H(2)	1.592	1.592	1.593	1.591	1.590	1.591
Ir−H(3)	1.843	1.838	1.832	1.797	1.794	1.791
Ir−H(4)	1.843	1.838	1.832	1.797	1.794	1.791
H(3)−H(4)	0.817	0.819	0.821	0.842	0.844	0.846

[a] See Figure 3 for the numbering of atoms.

Table 4. Activation Parameters (kcal/mol) for the Rotation of the Dihydrogen Ligand in $IrXH_2(\eta^2\text{-}H_2)(PR_3)_2$ (X = Cl, Br, I; R = H, Me)[a]

	R = H		R = Me		R = Pr^i
X	ΔE	$\Delta(E + ZPE)$	ΔE	$\Delta(E + ZPE)^b$	E_a
Cl	2.44	2.04	0.77	0.37	0.51[c]
Br	2.53	2.11	0.84	0.42	0.48[d]
I	2.75	2.32	1.09	0.66	1.00[e]

[a] ΔE is the electronic energy difference between the transition state and the reactant. [b] The zero-point energy corrections are taken from analogous model systems with PH_3 as a model phosphine. [c] The experimental value from ref 18. [d] The experimental value from the present work. The barrier for the Br is insignificantly smaller than that for the Cl despite the smaller rotational tunnel splitting because of the smaller value of *B* for the Br than the Cl compounds. [e] The experimental value from ref 9c.

in the rotational transition state than in the molecular hydrogen complex regardless of which model phosphine is used (compare Table 2 with Table 3). Moreover, it is interesting to note that from Cl to I the increase of the $Ir-H_2$ interaction in the molecular hydrogen complexes is relatively larger than that in the rotational transition states. This result accounts for the increasing rotational barriers along the halide series, as shown in Table 4. From Table 4, we find that, if the zero-point energy (ZPE) corrections obtained from PH_3 as a model phosphine are added to corresponding electronic energy differences obtained with the use of PMe_3, the calculated barriers are in remarkable accord with the related experimental values from previous studies on X = Cl[18] and I[9c] and from this study on X = Br. In contrast, the calculated rotational barrier with PH_3 as a model phosphine is much too large and beyond the experimental range. Because the rotational barrier is very sensitive to the nature of the phosphine, the use of PMe_3 as a model phosphine is critical for the quantitative estimate of the barrier to rotation of the molecular hydrogen.

Site Exchange Mechanism. As the temperature is increased the tunneling transitions broaden, shift to slightly lower frequencies, and decrease in intensity while a very broad background appears underneath these peaks, in much the same way as was observed for $RuH_2(\eta^2\text{-}H_2)_2(PCy_3)$.[13b] In addition, at temperatures greater than 100 K the narrow elastic line can be seen to broaden progressively. This indicates that another dynamic process is now fast enough to be observable with the frequency window (i.e. energy resolution) provided by the spectrometer of about 2 cm^{-1} fwhm. While the intensity of the quasielastic component is rather low, we were able to extract it by fitting a Lorenztian convoluted with the measured Gaussian resolution function over this part of the spectrum. An example of this procedure is shown in Figure 4 for $IrClH_2(\eta^2\text{-}H_2)(PPr^i_3)_2$ at 250 K. An effective activation energy for this line broadening can be obtained by fitting these Lorentzian widths to an Arrhenius law with the

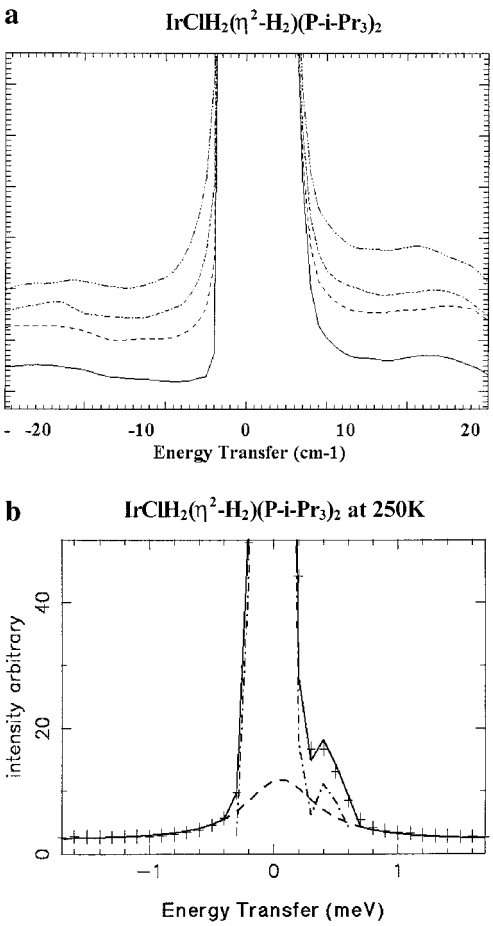

Figure 4. (a) Temperature dependence of the quasielastic line for $IrClH_2(\eta^2\text{-}H_2)(PPr^i_3)_2$, T = 100, 175, 210, and 250 K. Broadening is evident above 175 K in the base of the line. (b) Example of a fit to the data at T = 250 K. The line appears to be asymmetric because of a strong spectrometer-related "peak" at ca. 2 cm^{-1}.

result E_a = 1.5(2) kcal/mol. We associate this line broadening with the site exchange process for reasons discussed below.

To survey the three different mechanisms proposed in Scheme 1, we focus on the model system $IrXH_2(\eta^2\text{-}H_2)(PR_3)_2$ (X = Cl; R = H). It is reasonable to assume that the favored mechanism for X = Cl and R = H will be favored for the whole halide series with R = H or Me. Then, the optimized geometries of reactants (products and reactants are identical), intermediates, and transition states and the corresponding activation parameters are determined for the other model complexes only along the favored pathway.

The search for a possible intermediate on path A with X = Cl and R = H as a model phosphine results in the desired intermediate, i.e., the tetrahydride complex. This tetrahydride intermediate (Figure 5) was found to be only 4.3 kcal/mol higher in energy than the molecular hydrogen complex and was confirmed by numerical frequency calculations to be a true minimum. A search for a transition state between this tetrahydride intermediate and the reactant yielded a species which has one imaginary frequency and is less than 1.0 kcal/mol in energy above the intermediate. This late transition state, TS_{SE}, is structurally similar to the intermediate except for a shorter H(3)−H(4) distance (Figure 5).

B3LYP optimizations with X = Cl and R = H found no minima on paths B and C. After restricting the H−H distances of the two dihydrogen ligands in the hypothetical bis(dihydrogen) complex to 0.82 and 1.10 Å, the partial B3LYP optimiza-

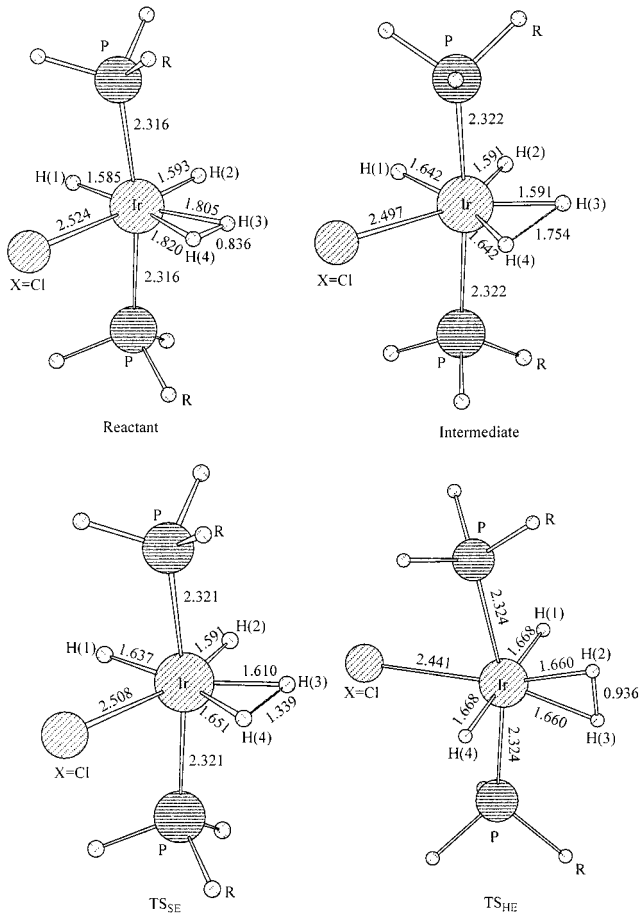

Figure 5. B3LYP/BS4-optimized structures for the reactant, the intermediate, and the two transition states, TS_{SE} and TS_{HE}, involved in the dihydrogen/hydride interchange process of $IrXH_2(\eta^2\text{-}H_2)(PR_3)_2$ (X = Cl; R = H).

tions give two structures which are 36.6 and 21.2 kcal/mol, respectively, above the reactant. Upon relaxing the H−H restriction in the geometry optimization, these species return to the above-mentioned tetrahydride intermediate. Additionally, rotating either or both H_2 ligands by 90° did not produce minima. In an analogous way (H(2)−H(3) bond distance fixed at 0.85 Å), a hypothetical intermediate on path C was found to be about 15.6 kcal/mol higher in energy than the reactant; this species also returned to the tetrahydride upon optimization. However, when the H(2)−H(3) bond was turned perpendicular to the Cl−H(1)−H(4) plane as a starting point, a full optimization resulted in a true stationary point, TS_{HE}, 21.6 kcal/mol above the reactant (Figure 5). By a frequency analysis, it was identified as a transition state for the direct exchange of H(2) and H(3) in the tetrahydride intermediate. Thus, the site exchange between H(2) and H(3) in the tetrahydride complex is unlikely to occur at lower temperatures since the corresponding barrier is 17.3 kcal/mol (21.6 − 4.3).

Summarizing the results above, one can conclude that only pathway A is possible for the site exchange process observed experimentally.[15] The low barrier on this pathway and the high barrier to H's crossing the Cl−Ir−P plane are consistent with the experimental observations.

With R = H, the structural parameters for intermediates and corresponding transition states along pathway A for the whole halide series have been collected in Table 5, and their relative energies reported in Table 6. The energies and geometries show that the exchange transition state is a very "late" transition state for all halides (the oxidative addition of the molecular hydrogen

Table 5. Selected B3LYP/BS4 Optimized Geometrical Parameters for the Intermediate and the Transition State TS_{SE} Involved in the Site Exchange Process of $IrXH_2(\eta^2\text{-}H_2)(PH_3)_2$ (X = Cl, Br, I)[a]

	TS_{SE}			intermediate		
	X = Cl	X = Br	X = I	X = Cl	X = Br	X = I
Ir−X	2.508	2.660	2.831	2.497	2.650	2.822
Ir−P	2.321	2.322	2.322	2.322	2.322	2.322
Ir−H(1)	1.637	1.635	1.635	1.642	1.641	1.640
Ir−H(2)	1.591	1.592	1.594	1.591	1.593	1.596
Ir−H(3)	1.610	1.613	1.616	1.591	1.593	1.596
Ir−H(4)	1.651	1.650	1.649	1.642	1.641	1.640
H(3)−H(4)	1.339	1.344	1.344	1.754	1.755	1.763

[a] See Figure 5 for the numbering of atoms.

Table 6. Relative Energies (kcal·mol^{-1}) at the B3LYP/BS4 Level for the Intermediate and the Transition State TS_{SE} Involved in the Site Exchange Process of $IrXH_2(\eta^2\text{-}H_2)(PR_3)_2$ (X = Cl, Br, I; R = H)

	intermediate (R = H)		TS_{SE} (R = H)		TS (R = Pr^i)
X	ΔE	$\Delta(E + ZPE)$	ΔE	$\Delta(E + ZPE)$	E_a
Cl	4.27	3.79	5.01	3.74	1.5(2)[a]
Br	4.05	3.60	4.78	3.48	
I	3.59	3.11	4.37	3.07	

[a] The experimental value from the present work.

is nearly complete in the transition state). There are relatively small geometrical differences between the intermediates and transition states as the halides are changed. The exchange barrier decreases slightly along the halide series, paralleling the increase in the H(3)−H(4) distance of the molecular hydrogen complexes (see Table 2). As shown in Table 6, the electronic energy difference between the transition state and the intermediate is quite small (about 0.7 kcal/mol for X = Cl, Br and 0.8 kcal/mol for X = I). When the zero-point energy corrections are added to these energy differences, the intermediate is slightly higher in energy (0.04 to 0.12 kcal/mol) than the "transition state". Thus, the intermediate for R = H may not exist.

The site exchange mechanism given by pathway A can convincingly explain what has been observed from the single crystal ^{1}H NMR study of $IrClH_2(\eta^2\text{-}H_2)(PPr^i_3)_2$. It was found experimentally[15] that the facile rearrangement between dihydrogen and two hydrides does not scramble them between all four sites on the NMR time scale. Remembering that the site exchange process between H(2) and H(3) in the intermediate is not particularly facile with a calculated activation energy of 17.3 kcal/mol (without zero-point and thermal energy corrections), one concludes that pathway A correctly interprets the observation that the hydrides occur in distinct pairs which do not cross the Cl−Ir−P plane. However, the major difficulty we encounter by using R = H as a model of Pr^i is that the calculated exchange barrier is higher than the corresponding experimental values, which earlier were estimated to be "substantially under 3 kcal/mol"[15] and are now determined to be 1.5(2) kcal/mol as described in the beginning of this subsection.

The relatively high exchange barrier (X = Cl) calculated for R = H suggests that PH_3 may not be a good model for the experimental phosphine (R = Pr^i). In the Experimental and Computational Section, we have demonstrated that PMe_3 is better than PH_3 in mimicking the experimental phosphine ligand. However, the qualitative conclusions established with PH_3 as a model phosphine will remain valid upon replacement of PH_3 by PMe_3. Thus, for the case of PMe_3 we only reoptimized the intermediate and the transition state along pathway A for X = Cl, Br, and I (we did not reexamine the other pathways). Selected structural parameters are given in Table 7. Comparing

Table 7. Selected B3LYP/BS4-Optimized Geometrical Parameters for the Intermediate and the Transition State TS_{SE} Involved in the Site Exchange Process of $IrXH_2(\eta^2\text{-}H_2)(PMe_3)_2$ (X = Cl, Br, I)[a]

	TS_{SE}			intermediate		
	X = Cl	X = Br	X = I	X = Cl	X = Br	X = I
Ir−X	2.537	2.690	2.861	2.523	2.676	2.847
Ir−P	2.353	2.355	2.357	2.353	2.355	2.356
Ir−H(1)	1.634	1.633	1.634	1.644	1.642	1.641
Ir−H(2)	1.590	1.591	1.592	1.589	1.591	1.594
Ir−H(3)	1.614	1.618	1.620	1.589	1.591	1.594
Ir−H(4)	1.659	1.657	1.654	1.644	1.642	1.641
H(3)−H(4)	1.269	1.270	1.278	1.757	1.756	1.756

[a] See Figure 5 for the numbering of atoms.

Table 8. Relative Energies (kcal·mol^{-1}) at the B3LYP/BS4 Level for the Intermediate and the Transition State TS_{SE} Involved in the Site Exchange Process of $IrXH_2(\eta^2\text{-}H_2)(PR_3)_2$ (X = Cl, Br, I; R = Me)

	intermediate (R=Me)		TS_{SE} (R=Me)		TS (R = Pr^i)
X	ΔE	$\Delta(E + ZPE)$[a]	ΔE	$\Delta(E + ZPE)$[a]	E_a
Cl	1.88	1.40	3.14	1.87	1.5(2)[b]
Br	1.92	1.47	3.09	1.79	
I	1.79	1.31	2.95	1.65	

[a] The zero-point energy corrections are taken from analogous model systems with PH_3 as a model phosphine (from Table 6). [b] The experimental value from the present work.

Tables 2, 5, and 7, we note that for each halide the dihydrogen ligand in the reactant is bonded to the metal more strongly with PMe_3 than with PH_3, but little change is seen for the hydride part of the tetrahydride intermediate when replacing PH_3 with PMe_3. Thus, the late transition state would be expected to have a lower barrier with PMe_3.

Accordingly, it can be seen from Table 8 that the change of phosphine reduces the activation energies by about 1.9, 1.7, and 1.4 kcal/mol for X = Cl, Br, and I, respectively. Again, if the ZPE corrections obtained from PH_3 as a model phosphine are added to corresponding electronic energy differences listed in Table 8, we obtain approximate ZPE-corrected activation energies of 1.9, 1.8, and 1.7 kcal/mol for X = Cl, Br, and I, respectively. Obviously, the calculated activation energy for X = Cl is now in excellent accord with our new experimental value, vida supra. Therefore, we can see that the use of PMe_3 as a model phosphine improves the results significantly. Additionally, the PMe_3 ligand stabilizes the tetrahydride intermediate enough that it remains an intermediate for all halides even with approximate ZPE correction.

Although the B3LYP method yields very satisfactory activation energies for the dihydrogen/hydride interchange, it is also important to compare this method with other methods in which electron correlation effects are treated in different ways. With the B3LYP/BS4 geometries, we recomputed the electronic energies at the B3LYP, HF, MP2, MP3, MP4(SDQ),[21] CISD,[32] and CCSD[33] levels with the largest basis set (BS5) for the reactant, intermediate, and transition state involved in the hydrogen exchange process of $IrClH_2(\eta^2\text{-}H_2)(PH_3)_2$. The relative energies are collected in Table 9. First, we note that the addition of an f polarization function on Ir has little influence on the relative energies at the B3LYP level. Clearly, the results of the Møller−Plesset perturbation series are oscillating severely and therefore are not reliable. A comparison of HF results with CISD and CCSD values reveals that electron correlation strongly stabilizes the classical tetrahydride intermediate and its related transition state and, thus, considerably reduces the energy difference between the intermediate and the nonclassical reactant as well as the barrier to hydrogen exchange. Encouragingly,

Table 9. Electronic Energy Differences (kcal·mol^{-1}) at Various Electron Correlation Levels with the B3LYP/BS4 Geometries for the Intermediate and the Transition State (TS_{SE}) Involved in the Site Exchange Process of $IrClH_2(\eta^2\text{-}H_2)(PH_3)_2$

level	TS_{SE}	intermediate	theoretical level	TS_{SE}	intermediate
B3LYP/BS4	5.01	4.27	MP4(SDQ)/BS5	1.08	−0.37
B3LYP/BS5	4.75	3.88	CISD/BS5	6.16	5.17
HF/BS5	13.54	13.32	CCSD/BS5	2.64	1.27
MP2/BS5	−4.03	−5.93	CCSD(T)/BS5	1.06	−0.43
MP3/BS5	3.64	2.33			

the B3LYP results seem to lie between variational CISD and size-consistent CCSD values. Therefore, we conclude that the B3LYP energies for $IrXH_2(\eta^2\text{-}H_2)(PR_3)_2$ (X = Cl, Br, I; R = H, Me) are fairly accurate and that our agreement between calculated and experimental results is not fortuitous. Note that inclusion of triple excitations by perturbation theory, CCSD(T), overcorrects for electron correlation as has been seen in other cases where MPn methods also overcorrect.[39]

The above theoretical result for the activation energy for the site exchange (1.9 kcal/mol for X = Cl) is in excellent agreement with the results for the quasielastic broadening of the INS spectrum at high temperatures. While in principle a number of dynamic processes in this type of complex could give rise to such a broadening of the elastic line, we nonetheless can attribute this effect to the rapid interconversion between hydride and dihydrogen ligands. There are basically two reasons for this conclusion. First, reorientational motion of either the methyl groups on the phosphine or the phosphine itself is likely to be subject to much higher barriers (the barrier to methyl rotation should be close to that in propane, which has been determined to be 3.4 kcal/mol[40]) and/or governed by much smaller values of *B* for either process to be observable with the instrumental resolution used in this experiment. Second, the intensity of the quasielastic line roughly reflects the fact that at most four H's (the dihydrogen−dihydride ligands) participate in this process (with 42 H's on the phosphines), while for the other processes many more H are likely to be involved. We also have limited data on a sample with perdeuterated P−Pr^i ligands which still shows the broadening.

Finally, we note that the site exchange barrier is only about 1.0 kcal/mol higher than the corresponding rotational barrier. Therefore, our results do not exclude the possibility that the site exchange process and the rotation of the molecular hydrogen are coupled to some extent.[9c,18]

Conclusions

In this paper three different possible mechanisms for the intramolecular dihydrogen/hydride interchange in $IrXH_2(\eta^2\text{-}H_2)(PR_3)_2$ (X = Cl, Br, I; R = H, Me) have been examined by using density functional theory. Our B3LYP/BS4 calculations with X = Cl and R = H strongly support the oxidative-addition/reductive-elimination pathway through a tetrahydride intermediate as the most favored mechanism. With the more realistic phosphine, PMe_3, and with approximate ZPE corrections, the exchange barriers are found to be 1.9, 1.8, and 1.7 kcal/mol for X = Cl, Br, and I, respectively. For the latter system, the calculated activation energy for X = Cl is in excellent agreement with the related experimental value of 1.5(2) kcal/mol obtained from inelastic neutron scattering studies. Because the tetrahydride intermediate is only slightly more stable than the transition state connecting it to the molecular hydrogen compound, it may

(39) Niu, S.; Hall, M. B. *J. Phys. Chem. A* **1997**, *101*, 1360.
(40) McMurry, J. *Organic Chemistry*; Brooks/Cole Publishing Company: Pacific Grove, CA, 1996.

be difficult to detect this intermediate species. The direct oxidative-addition/reductive-elimination mechanism, as illustrated here, is one of several mechanisms that may be responsible for the fluxional behavior of other transition metal polyhydride complexes.[5f,10,11d−f]

The rotational barriers of the dihydrogen ligand in $IrXH_2(\eta^2\text{-}H_2)(PPr^i_3)_2$, both previously measured X = Cl and I values and the X = Br value reported here, are also well reproduced by our B3LYP/BS4 calculations on the model complexes $IrXH_2(\eta^2\text{-}H_2)(PMe_3)_2$ (X = Cl, Br, I). The use of PMe_3 as a model phosphine is again shown to be crucial for the quantitative estimate of the barrier to rotation of the dihydrogen ligand. In addition, our calculations also do not rule out the possibility that in the $IrXH_2(\eta^2\text{-}H_2)(PPr^i_3)_2$ (X = Cl, Br, I) complexes the site exchange process and the rotational motion of the dihydrogen ligand are coupled to some extent because their respective barriers are of similar magnitude.

Finally, generalization of the results presented here suggests that, if appropriate basis sets and model ligands are chosen, the density functional theory (specifically B3LYP) with effective core potentials is a reliable theoretical tool for elucidating the intramolecular exchange mechanisms and evaluating the rotational barrier of the molecular hydrogen in transition metal polyhydrides.

Acknowledgment. The authors thank the National Science Foundation (Grant No. CHE 9800184) and the Robert A. Welch Foundation (Grant No. A-648) for their generous support. They also thank the Institut Laue-Langevin and the Laboratoire Léon-Brillouin for use of their facilities. Work at Los Alamos National Laboratory was supported by the Office of Science, U.S. Department of Energy. Los Alamos National Laboratory is operated by the University of California under contract number W-7405-ENG-36 with the U.S. Department of Energy. The authors also thank MURST for their support.

JA993877A